Topology of Charge Density of Flucytosine and Related Molecules and Characteristics of their Bond Charge Distributions

Juan Murgich,*,† Héctor J. Franco,‡ and Gioconda San-Blas†

Centro de Química and Centro de Microbiología y Biología Celular, Instituto Venezolano de Investigaciones Científicas (IVIC), Apartado 21827, Caracas 1020A, Venezuela, and Escuela de Química, Facultad de Ciencias, Universidad Central de Venezuela, Caracas, Venezuela

Received: February 16, 2006; In Final Form: June 13, 2006

The molecular charge distribution of flucytosine (4-amino-5-fluoro-2-pyrimidone), uracil, 5-fluorouracil, and thymine was studied by means of density functional theory calculations (DFT). The resulting distributions were analyzed by means of the atoms in molecules (AIM) theory. Bonds were characterized through vectors formed with the charge density value, its Laplacian, and the bond ellipticity calculated at the bond critical point (BCP). Within each set of C═O, C−H, and N−H bonds, these vectors showed little dispersion. C−C bonds formed three different subsets, one with a significant degree of double bonding, a second corresponding to single bonds with a finite ellipticity produced by hyperconjugation, and a third one formed by a pure single bond. In N−C bonds, a decrease in bond length (an increase in double bond character) was not reflected as an increase in their ellipticity, as in all C−C bonds studied. It was also found that substitution influenced the N−C, C−O, and C−C bond ellipticity much more than density and its Laplacian at the BCP. The Laplacian of charge density pointed to the existence of both bonding and nonbonding maxima in the valence shell charge concentration of N, O, and F, while only bonding ones were found for the C atoms. The nonbonding maxima related to the sites for electrophilic attack and H bonding in O and N, while sites of nucleophilic attack were suggested by the holes in the valence shell of the C atoms of the carbonyl groups.

Introduction

Flucytosine (5-fluorocytosine or 4-amino-5-fluoro-2-pyrimidone) is the only available antimetabolite drug with known antifungal activity. Flucytosine is transported into sensitive cells and then converted to 5-fluorouracil by fungal cytosine deaminase.[1] It inhibits fungal protein synthesis by replacing uracil with 5-fluorouracil in the fungal RNA. Flucytosine is chemically a pyrimidine, and it is activated by deamination within the fungal cells to 5-fluorouracil. Flucytosine is quite active against many fungi, among them, *Candida* spp., *Cryptococcus neformans*, *Aspergillus* spp., and the dematiaceous fungi *Phialophora* spp. and *Cladosporium* spp.[2]

The detailed chemical mechanism of flucytosine action is not well-known, and information about its electronic distribution and that of uracil, 5-fluorouracil, and thymine may help in the determination of some of the chemical pathways involved in its therapeutic action. Chemical properties are related to the molecular electronic charge distribution $\rho(\mathbf{r})$.[3,4] Therefore, it is important to first characterize this distribution in a way that comparisons of similar molecules can be readily made. As rearrangements of the covalent bonds are expected to occur, it is of interest to compare the charge distribution of different bonds present in these molecules. This will provide a background upon which comparisons could be made once the chemical pathway becomes known in detail. In this work, the $\rho(\mathbf{r})$ of flucytosine, uracil, 5-fluorouracil, and thymine (Figure 1) were calculated by means of the density functional theory (DFT) using a B3YLP hybrid functional with a large basis set (6-311G(3d, 2p)). The topology of $\rho(\mathbf{r})$ for these molecules was studied, and the results were interpreted by means of the atom in molecules (AIM) theory.[3,4] The bond and valence shell charge distribution VSCC extremes were determined and characterized for the C, N, O, and F atoms. The charge distribution of the different bonds was studied at the bond critical point BCP as defined by the AIM theory. This allowed us to test the classical assumption relating the variations of the degree of double bonding produced by changes in bond length with the charge and its asymmetry around the bond axis at the BCP. The C−C bonds were found to show a wide distribution in their bond lengths. This is generally interpreted as a result of variations in their double bond character. The C−C bonds showed an excellent correlation between the charge density and its ellipticity at the BCP. In N−C bonds, a shortening in bond lengths (increase in double bond character) that is reflected in an increase in $\rho(\mathbf{r})$ at the BCP was not followed by an increase in their ellipticity, as in all C−C bonds studied in this work. The same behavior was also found in similar C−C and C−N bonds present in several F derivatives of azidothymidine. Results obtained at the BCPs showed that the C═O, N−H, and C−H bonds exhibited little changes upon substitution. In the C═O bonds, the symmetry of the molecular surroundings influenced somewhat its charge distribution at the BCPs. Also, it was found that substitution influenced the N−C, C═O, and C−C bond ellipticity much more than the density and its Laplacian at the BCP. From the study of the surface of the Laplacian of $\rho(\mathbf{r}) = 0$, information about the nucleophilic and electrophilic attack sites and intermolecular H bonds were also obtained for these molecules. In particular, the carbonyl groups showed a remarkable similarity surface with the same groups found in urea and

* Corresponding author e-mail: jmurgich@ivic.ve.
† Instituto Venezolano de Investigaciones Científicas (IVIC).
‡ Universidad Central de Venezuela.

10.1021/jp061007r CCC: $33.50 © 2006 American Chemical Society
Published on Web 07/29/2006

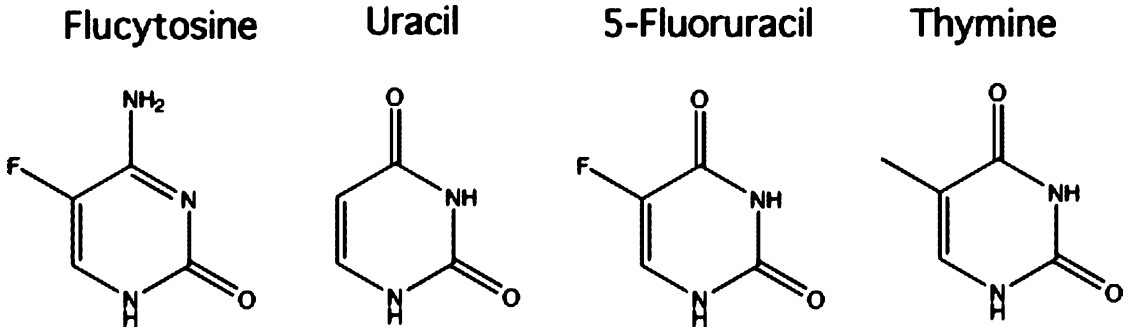

Figure 1. Molecular structures of flucytosine (tot. energy = −494.33404 au), uracil, (tot. energy = −414.85341 au), 5-fluorouracil (tot. energy = −514.22484 au), and thymine (tot. energy = −454.18409 au).

methanal. This shows that all these groups will have similar chemical reactivity.

Computational Methods

Molecules were built with GaussViewM 03 and optimized with Gaussian 03M[6] employing a hybrid B3YLP functional.[5] All the molecular structures were optimized with the 6-31G(d) basis set. The sensitivity of the magnitudes related to derivatives of the charge density with the basis set employed led to the use of a larger one in their calculation. Then, a single point calculation employing the optimized structure was done for each molecule with the same functional although with a much larger 6-311G(3d,2p) basis set. These types of calculations have been used in recent works on the topology[4] of $\rho(\mathbf{r})$ because it ensures a reasonable compromise between the wave function quality required to obtain reliable values of the derivatives of $\rho(\mathbf{r})$ and the computer power available. Electron density $\rho(\mathbf{r})$, gradient vector field $\nabla\rho(\mathbf{r})$, associated Laplacian $\nabla^2\rho(\mathbf{r})$, critical points in $\rho(\mathbf{r})$, interatomic surfaces, and bond paths were determined with a local version of the program Morphy 95[7] and, in some cases, also with Morphy 98.[8] Atomic charges $q(\Omega)$ were determined with the program PROAIM 94.[9]

Theory

The electron density in a molecule is dominated by the distribution around the nuclei.[3,10] A small value in comparison with the $\rho(\mathbf{r})$ at the nuclei ($\leq 1\%$) is found in the region located between covalently bonded atoms except for hydrogen.[3] It is interesting to mention that the $\rho(\mathbf{r})$ of a molecule is almost equal to that generated by the superposition of noninteracting atoms. Bond formation is just a small perturbation in $\rho(\mathbf{r})$ of the individual free atoms. Therefore, to characterize the molecular $\rho(\mathbf{r})$, methods that provide an enhanced view of them are required. Bader and co-workers[3−5,10] found that the application of differential operators to $\rho(\mathbf{r})$ provided that enhancement. With their use, the molecule is partitioned into well-defined 3D regions by means of features that are directly related to $\rho(\mathbf{r})$.[3−5] The distribution of all $\nabla\rho(\mathbf{r})$ path determines the way in which a molecule is partitioned in atoms. A gradient path moves in the direction of steepest ascent in $\rho(\mathbf{r})$ until it reaches an attractor point, which in most cases coincides with a nucleus.[3−5] The set of all gradient paths attracted to one nucleus constitutes an atomic basin. Such a basin is a portion of space that takes a unique shape dictated by the nature of its neighboring atoms.[3−5] Therefore, these atomic regions or basins of volume Ω are not arbitrary and provide a unique definition of atoms in molecules.[5]

The Topology of the Molecular Charge Distribution

The topological properties of a scalar field such as $\rho(\mathbf{r})$ are summarized in terms of their critical points,[4,5] i.e., the points $\mathbf{r}_c$ where $\nabla\rho(\mathbf{r}_c) = 0$. Critical points are classified according to their type (m, n) by stating their rank m and signature n. The rank is equal to the number of nonzero eigenvalues of the Hessian matrix of $\rho(\mathbf{r})$ at $\mathbf{r}_c$, while the signature is the algebraic sum of the signs of the eigenvalues of this matrix.[3] Critical points of (3, −1) and (3, +1) type describe saddle points, while the (3, −3) is a maximum in the field. The interaction of two atoms in a molecule leads to the formation of a (3, −1) bond critical point (BCP) in $\rho(\mathbf{r})$, and the gradient paths that originate and conclude at this point serve to define the bond path (BP) and the interatomic surface[3,4] (IAS), respectively. Any IAS is such that it is a zero flux surface for $\nabla\rho(\mathbf{r})$. The three eigenvalues of the Hessian matrix represent the local curvatures of $\rho(\mathbf{r})$ at the critical point, while the associated eigenvectors show their directions in space. The asymmetry in the curvatures of $\rho(\mathbf{r}_c)$ λ_1 and λ_2 in the directions perpendicular to the bond at the BCP is described by the ellipticity[3] $\epsilon = (\lambda_1/\lambda_2) - 1$. The values of ϵ measure the deviation of the charge distribution of a bond path from axial symmetry.[4,5,10] The ellipticity provides, then, a measure of the double character of a bond.

The Laplacian field allows not only the recovery of the chemical model of the localized bonded and nonbonded electron pairs but also the characterization of local concentrations [$\nabla^2\rho(\mathbf{r}) < 0$] and depletions [$\nabla^2\rho(\mathbf{r}) > 0$] of the electronic density.[3,4,10] In fact, the $\nabla^2\rho(\mathbf{r})$ distribution for a free atom ($Z < 40$) reflects the quantum shell structure by exhibiting the corresponding number of alternating pairs of shells of charge concentration and depletion. Upon bonding, local maxima and minima are formed in the valence shell of a bonded atom, and their number, type, location, and value of $\nabla^2\rho(\mathbf{r})$ are a function of the atoms linked to it.[3,4,10]

The critical points characterize the $\rho(\mathbf{r})$ of a molecule in a nonarbitrary way. Comparisons between the $\rho(\mathbf{r})$ of molecules or atomic groups using these points can then be made without any ambiguities, and subtle differences can be easily identified. The $\rho(\mathbf{r}_c)$, $\nabla^2\rho(\mathbf{r}_c)$, and ϵ values may be considered the components of a chemical descriptor vector.[11] Each vector describes a bond in a three-dimensional abstract BCP space of the molecule.[11] Hence, the use of the BCP space allows an accurate comparison of the charge distributions for different molecules or atomic groups.

Substituent Effects

The electronic effects of a substituent X in molecules originate from three main processes:[12] (1) the charge redistribution produced by the dipole polarization and/or net charge of X, generating a field effect; (2) the electronegative difference between X and the atom to which it is attached, producing a transfer toward the more electronegative one (σ-inductive or electronegativity effect); and (3) the charge transfer between

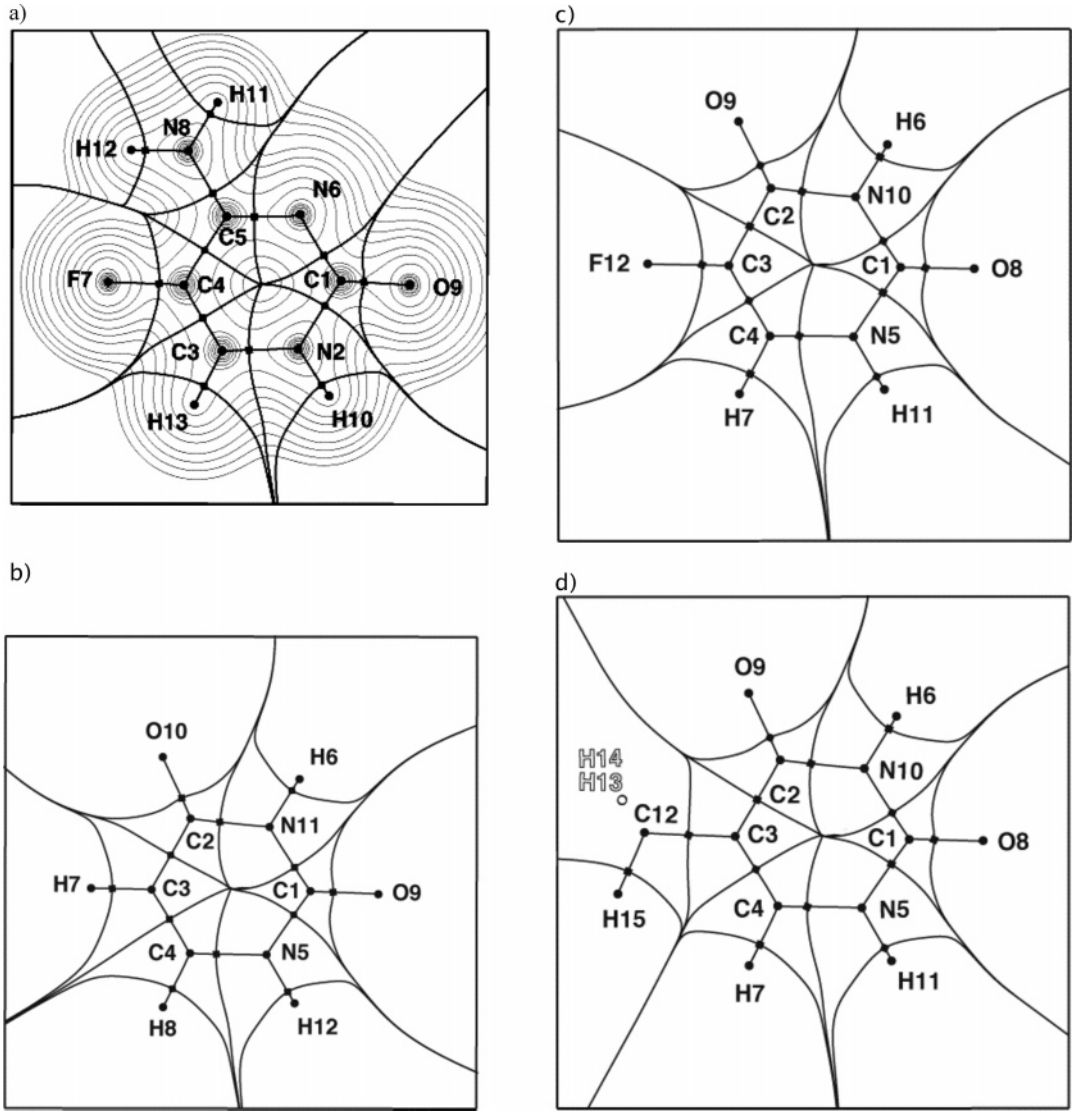

Figure 2. The bond paths, bond critical points, and interatomic surfaces (in bold) superimposed on the electron density isocontour lines in the molecular plane of (a) flucytosine. The same but without the contour lines for (b) uracil, (c) 5-fluorouracil, and (d) thymine.

proper π orbitals of X and those of the group to which it is attached, generating the resonance effect. The field effect, involving a direct through space interaction, is the main mechanism of transmission where one or more atoms separate the probe center[12] from X. This effect arises from the dipole polarization or net charge of X as felt elsewhere in the molecule at probe site. The field effects are dependent on the size and geometry of the dipole polarization and/or net charge of X with respect to the probe. The other mode of transmission is the progressive but fast diminishing relay of polar effects along a chain of atoms.[12] Such effects originate in the electronegativity difference between substituent X and the atom to which it is attached. Thus, the inductive effects depend on the atomic/group electronegativity of X. In turn, the resonance effect also depends on the ability of X to accept or donate electronic charge to an adjacent atom or group.[12]

Results and Discussion

The structures of molecules studied in this work are shown in Figure 1. Each atomic basin is separated from the rest of the space by IASs.[3,4,10] Parts (a)−(d) of Figure 2 show their intersection with the molecular plane that contain the nuclei. A comparison of O10 atomic basin in uracil [Figure 2(b)] with that of O9 in 5-fluorouracil [Figure 2(c)] showed that the F atom influences the shape of IAS of this neighboring carbonyl group. The same effect is observed when the IASs of O8 and O9 in 5-fluorouracil [Figure 2(c)] are compared. In this case, O8 showed a symmetrical basin in the molecular plane, while in O9 the F atom has displaced the IAS toward the neighboring basin. A similar effect is observed in thymine where a methyl group perturbs the IAS of the O9 atom [Figure 2(d)] or in flucytosine, where the amine group modifies the F basin [Figure 2(a)]. These results show that the IAS is quite sensitive to the nearest atoms or groups present in the molecule. Similar conclusions may be obtained for IASs from other atoms present in flucytosine and related molecules.

Figure 2 also shows all bond paths and (3,−1) bond critical points for flucytosine and related set of molecules. BCP properties are shown in Table 1. A (3,+1) ring critical point is also found at the ring center of each molecule.[3,4] Nevertheless, little information can be drawn from it, and, therefore, they were not displayed or further analyzed.

The BCP space allows the quantitative comparison of one given type of bond present in different molecules. The subtle electronic redistributions produced by a substituent and other effects on the BCP may be easily studied. In flucytosine, the

TABLE 1: Properties of the Bond Critical Points and Bond Lengths

flucytosine									
	bond								
property	C1−N2	C1−N6	C4−C5	C5−N6	C1−O9	C3−N2	C3−C4	C4−F7	C5−N8
length	1.428	1.378	1.439	1.316	1.219	1.362	1.351	1.357	1.354
$\rho(\mathbf{r}_c)$	0.284	0.326	0.297	0.370	0.427	0.323	0.346	0.258	0.333
$\nabla^2\rho(\mathbf{r}_c)$	−0.814	−1.019	−0.819	−1.225	−0.693	−0.990	−1.054	−0.036	−1.089
ϵ	0.141	0.127	0.218	0.162	0.161	0.141	0.415	0.097	0.169
uracil									
	bond								
property	C2−N11	C1−N5	C4−N5	C1−N11	C3−C2	C1−O9	C3−C4	C2−O10	
length	1.409	1.391	1.370	1.380	1.456	1.208	1.343	1.210	
$\rho(\mathbf{r}_c)$	0.295	0.312	0.315	0.320	0.287	0.438	0.346	0.432	
$\nabla^2\rho(\mathbf{r}_c)$	−0.884	−0.991	−0.943	−1.025	−0.766	−0.651	−1.060	−0.578	
ϵ	0.108	0.167	0.086	0.182	0.150	0.146	0.333	0.125	
5-fluorouracil									
	bond								
property	C2−N10	C1−N5	C4−N5	C1−N10	C1−O8	C2−C3	C3−C4	C2−O9	C3−F12
length	1.403	1.386	1.376	1.386	1.207	1.461	1.340	1.207	1.331
$\rho(\mathbf{r}_c)$	0.299	0.314	0.311	0.315	0.438	0.289	0.353	0.435	0.277
$\nabla^2\rho(\mathbf{r}_c)$	−0.904	−1.002	−0.931	−0.997	−0.651	−0.781	−1.091	−0.550	−0.020
ϵ	0.125	0.181	0.115	0.179	0.149	0.205	0.429	0.128	0.059
thymine									
	bond								
property	C2−N10	C1−N5	C4−N5	C1−N10	C1−O8	C3−C2	C3−C4	C2−O9	C12−C3
length	1.403	1.385	1.375	1.381	1.209	1.465	1.345	1.212	1.497
$\rho(\mathbf{r}_c)$	0.298	0.316	0.311	0.318	0.437	0.283	0.345	0.423	0.256
$\nabla^2\rho(\mathbf{r}_c)$	−0.905	−1.000	−0.923	−1.020	−0.659	−0.741	−1.046	−0.579	−0.611
ϵ	0.113	0.180	0.098	0.180	0.146	0.150	0.346	0.121	0.048

C═O bond values of $\rho(\mathbf{r})$, $\nabla^2\rho(\mathbf{r})$, and ϵ at the BCP were remarkably similar to those found for this atomic group in the other molecules [Figure 3(a)]. The BCP vectors of the C═O bond were so close that only four out of the seven vectors can be distinguished in this graph. The compactness of the C═O vector cluster showed that the bonding in this group maintains essentially the same electronic density at the BCP. Only minor perturbations produced by modifications in other parts of the molecule are present in the carbonyls for this set of molecules. The small variations found in the atomic charges for the C2 and O(9 or 10) pair of the C═O bonds next to the substitution site shows the constancy of $\rho(\mathbf{r})$ in this group upon substitution (see Table 1). The ellipticity of the C−O bond was relatively constant for the carbonyl group more distant from the substitution site ($\epsilon\sim0.15$) in uracil, thymine, and 5-fluorouracil. In the second carbonyls of these molecules, ϵ was slightly lower (~0.12), while in flucytosine its value rose to 0.16. Then, the ellipticity at the C═O BCP seems to be more sensitive to the changes in its neighboring atoms than $\rho(\mathbf{r}_c)$ or $\nabla^2\rho(\mathbf{r}_c)$ because it showed some significant variations ($\sim25\%$) upon substitution.

BCP vectors for the nine C−C bonds of flucytosine and related molecules are shown in Figure 3(b). There are three distinct clusters for these bonds reflected in their lengths. One associated with bonds with high values of both ϵ and $\rho(\mathbf{r})$ that corresponds to C−C double bonds (Figure 1). A second set related to an intermediate bond with a reduced although finite ellipticity. This latter set has an average $\rho(\mathbf{r}_c)$ value close to that of a classical single C−C bond (~0.260 au) with an asymmetry in its distribution, generated by the delocalization of neighboring double bonds via resonance.[12,13] Instead of having $\epsilon = 0$, as in a single C−C bond, the delocalization from neighboring double bonds generates a finite ellipticity [Figure 3(b)] in them.[13] This set contains the remaining C−C bonds of the different rings in Figure 1, except for one of the methyl groups in thymine (C3−C12). This one showed a $\rho(\mathbf{r})$ value similar to that of an almost pure single C−C bond with a very low ϵ value (0.040). Then, the C−C bonds of the different molecules in Figure 3(b) cover a wide range of values, from a pure single to a double bond.

BCP vectors for the different C−H and N−H bonds were found to cluster very tightly within each set (for N−H bonds, see Figure 3(c)). They showed the same trend as found for the C═O bonds. This close clustering indicates both a strong similarity among the charge densities within each set of bonds and little sensitivity toward changes produced by substitution. The average values for N−H bonds were as follows: $\rho(\mathbf{r}_c) = 0.349 \pm 0.003$, $\nabla^2\rho(\mathbf{r}_c) = -1.89 \pm 0.03$, and $\epsilon = 0.045 \pm 0.004$, while those of C−H bonds were $\rho(\mathbf{r}_c) = 0.287 \pm 0.007$, $\nabla^2\rho(\mathbf{r}_c) = -1.06 \pm 0.06$, and $\epsilon = 0.020 \pm 0.005$. C═O bond values were as follows: $\rho(\mathbf{r}_c) = 0.433 \pm 0.006$, $\nabla^2\rho(\mathbf{r}_c) = -0.62 \pm 0.05$, and $\epsilon = 0.14 \pm 0.02$. As expected, $\rho(\mathbf{r}_c)$ values showed the least variation, while both the Lapacian and the ellipticity showed the largest deviations due to the sensitivity of the second derivatives to small changes in the charge density. (Values for the N−H and C−H bonds are available from the authors upon request.)

BCP vectors for N−C bonds exhibited, instead, a noticeable scattering in the resulting cluster [Figure 3(d)]. For this type of bond, $\rho(\mathbf{r}_c)$ does not seem to increase with the ellipticity of the N−C bonds [Figure 4(a)]. A linear regression ($\rho = 0.196\epsilon + 0.287$ with $r^2 = 0.127$) showed the lack of correlation between $\rho(\mathbf{r}_c)$ and ellipticity in these N−C bonds. Instead, it found an excellent one for the C−C bonds ($\rho = 0.268\epsilon + 0.243$ with $r^2 = 0.954$) of the same set of compounds [see Figure 4(b)]. A

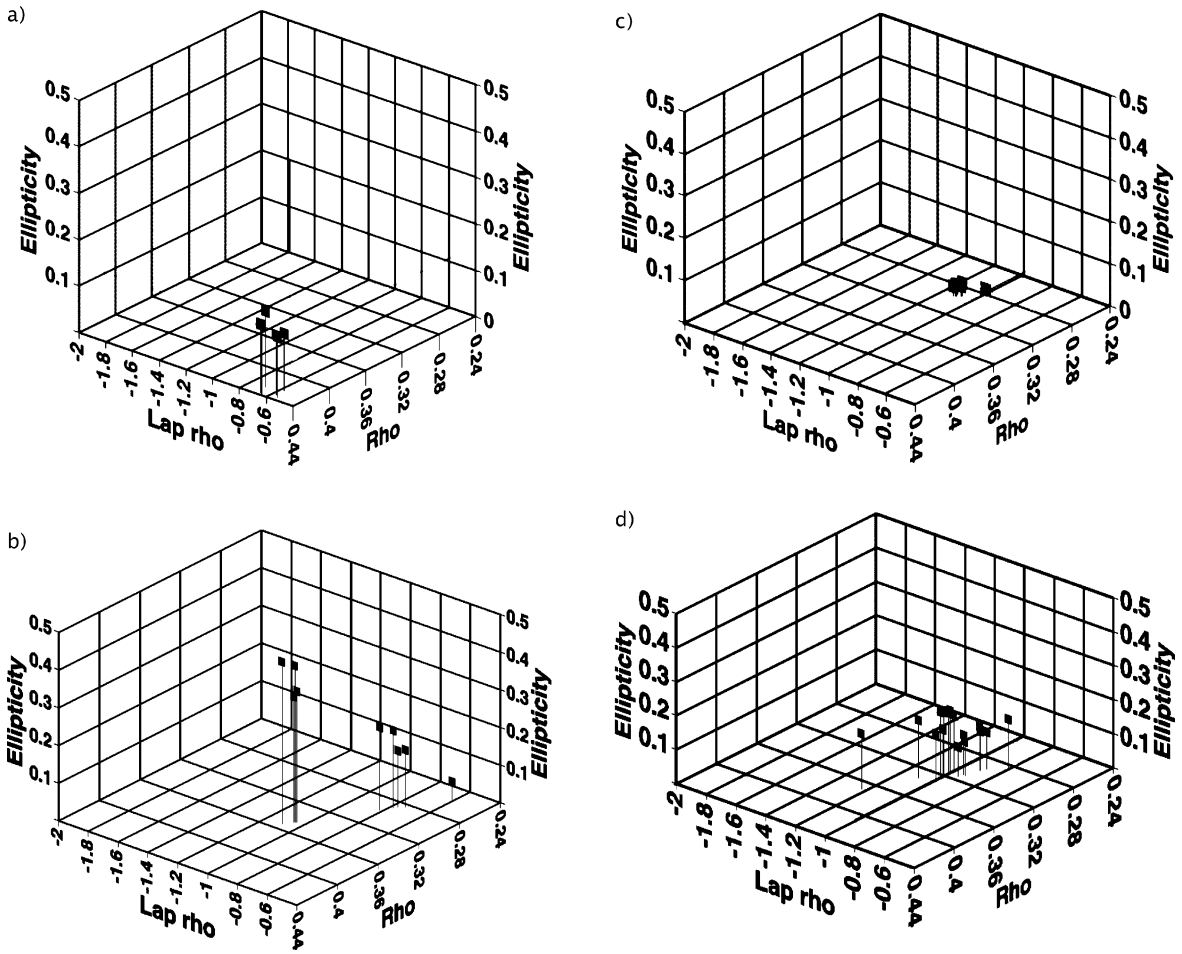

Figure 3. Vectors in the BCP space for (a) the C═O bonds, (b) the C−C bonds, (c) the N−H bonds, and (d) the N−C bonds present in flucytosine and related molecules.

comparison of Figure 4(a),(b) shows that the same variation in $\rho(\mathbf{r}_c)$ produces a much larger response in ellipticity in C−C than in N−C bonds. A similar trend was found for the C−C and C−N bonds present in several F derivatives[14] of AZT (3′-azido-3′-deoxythymidine). In these compounds, again the C−C bonds showed an excellent correlation between $\rho(\mathbf{r}_c)$ and ϵ ($r^2 = 0.977$). However, the N−C bonds exhibited a noticeable lower correlation ($r^2 = 0.735$) although with an *opposite* slope than in the C−C bonds. The resulting slope in the F-AZT C−N bonds is such that an increase in $\rho(\mathbf{r}_c)$ will *decrease* the ellipticity at the critical point of the C−N bond. This means that a decrease in the CN bond length produces changes in $\rho(\mathbf{r}_c)$ that are quite different from those found in CC bonds. In the latter ones, a decrease in bond length that is classically interpreted as an increase in double bond character is associated with an increase in *both* density and ellipticity at the BCP. This increase is brought about by charge accumulation in a plane containing the bond path and, in our case, perpendicular to the molecular plane. In the CN case, additional factors such as external fields seem to influence the values of ϵ at the BCP when the bond length is varied. To further explore the behavior of these bonds upon variations in length, the correlation between $\rho(\mathbf{r}_c)$ and the corresponding bond length was studied. For the CC case, an excellent correlation was found, ($\rho(\mathbf{r}_c) = -0.557$ bond length (Å) + 1.097 with $R^2 = 0.989$), while for the CN only a reasonable one was obtained, ($\rho(\mathbf{r}_c) = -0.903$ bond length (Å) + 1.560 with $R^2 = 0.872$). In this case, the charge distribution in the CN and in the CC bonds behave similarly when the bond length is varied and, in every case, a decrease in length brings about an increase in $\rho(\mathbf{r}_c)$ and vice versa. The response of $\rho(\mathbf{r}_c)$ upon changes in the CN bonds showed no unexpected behavior in contrast with the variations found for the ellipticity. Again it is found that $\rho(\mathbf{r}_c)$ is much less sensitive to changes[3,4] than its derivatives and, consequently, does not reflect in the same way small changes that markedly influence the ellipticity through the small variations in the curvatures. It is then not surprising that the relationship found between $\rho(\mathbf{r}_c)$ and ϵ for the C−C bonds when the bond length (double bond character) changes is not valid for the N−C bonds. Then, ϵ is not a reliable measure of bond order, and other parameters such as the electron pair density should be used to properly define it.[15]

Substituent Effects

It is interesting to explore the electronic effects[12] of substituting H7 in uracil by a charge-withdrawing F atom or a donating $-CH_3$ group on the neighboring C2−C3 and C3−C4 bonds. A comparison of $\rho(\mathbf{r}_c)$, $\nabla^2\rho(\mathbf{r}_c)$, and ϵ for uracil, 5-fluorouracil, and thymine (Table 1) showed that the substitution of H7 by a F atom or a methyl group produces only marginal changes ($\leq 5\%$) in both $\rho(\mathbf{r}_c)$ and $\nabla^2\rho(\mathbf{r}_c)$ of the neighboring C3−C4 and C3−C2 bonds. As a consequence, the transmission of electronic effects produced by the F substitution diminishes very quickly along a chain of C atoms in a ring.[12] Charge distribution at the C3 atom in uracil is drastically modified by F substitution [Figure 2(b)−(d)]. This is mainly reflected in changes at the C3 portion of the IAS facing the F atom in 5-fluorouracil. The IAS portion between F and C3 atoms is significantly displaced toward the C atom, as expected from their marked differences in electronegativity.[3] Nevertheless, the other two C3 IASs

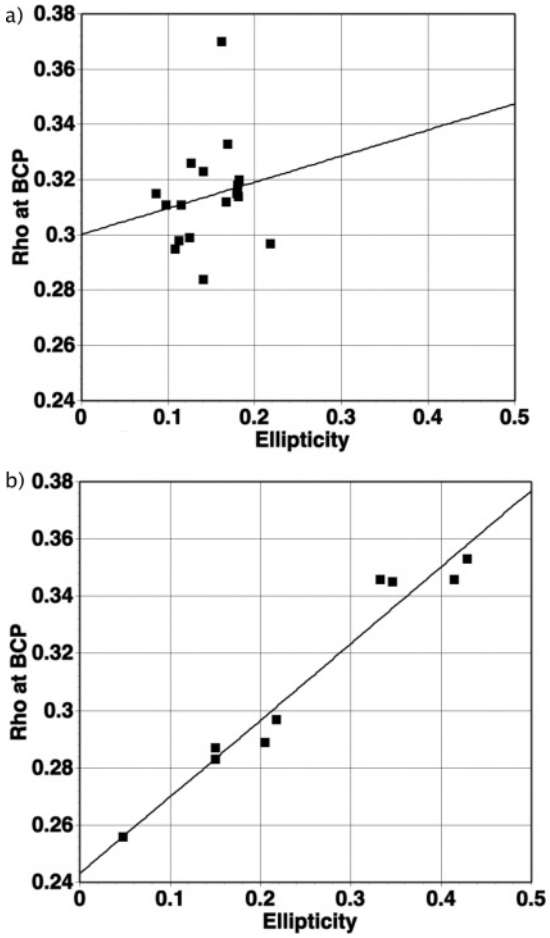

Figure 4. Charge density at the BCP (ρ at BCP) versus the bond ellipticity for (a) the N−C bonds and (b) the C−C bonds in flucytosine and related molecules.

(facing C2 and C4 atoms) are only slightly perturbed by such F substitution (Figure 2(c)). Then, this C atom seems capable of adjusting its VSCC on the substituent side without significantly modifying the IAS portions facing the two C−C bond directions. This suggests that the primary effects of bonding in this type of C atoms are a rather local process in terms of charge distribution of their valence shell.

Atomic charges $q(\Omega)$ of C2 and C4 were only slightly changed upon substitution (2 and 5%, respectively). Instead, in C3, changes were more significant (Table 3). From a slightly negative charged C3 (−0.009e) in uracil, it passes to a strongly positively charged atom (+0.566e) in 5-fluorouracil. In thymine, instead, the C3 charge is only slightly modified (+0.026e), as expected from the small differences in electronegativities between C and H. Variations in the atomic charges showed that the main effect of the substitution in uracil is concentrated mainly in the C3 basin with only small changes in the C2 and C4 atoms. Nevertheless, upon substitution, a change of 23% (−F) and 27% ($-CH_3$) with respect to uracil was found in the ellipticity of the C3−C2 and C3−C4 bonds. These changes in ϵ are generated by only a 6 and 4.7% increase, respectively, in λ_1 and a decrease in λ_2 of less than 2%. This shows that the curvatures perpendicular to the C−C bond path at the BCP are noticeably more sensitive to substitution than values of $\rho(\mathbf{r}_c)$, $\nabla^2\rho(\mathbf{r}_c)$, or atomic charges. The origin of this sensitivity may be found in the fact that the minute changes produced by i.e., the field effect on $\rho(\mathbf{r}_c)$ are remarkably amplified when second derivatives such as the bond transverse curvatures are considered.[4]

$\nabla^2\rho(\mathbf{r})$ Distribution and Valence Shell Charge Concentration

Figure 5(a)−(d) shows the distribution of $\nabla^2\rho(\mathbf{r})$ in the nuclear plane of the molecules of interest and the maxima (at the nuclei) and saddle (at the bonds) critical points in $\rho(\mathbf{r})$. Molecular coordinates and $\rho(\mathbf{r})$ and $\nabla^2\rho(\mathbf{r})$ values for the maxima found in the valence shells of N, O, and F atoms are found in Table 2.

In flucytosine, a typical amidic N atom N2 presented three bonded maxima in the VSCC, one along the direction of the N2−H10 bond and one along each of the N2−C bonds (Figure 5a). Such maxima were all found in the molecular plane. Similarly to urea,[3] two additional nonbonding maxima were found in the valence shell of N2, one above and the other below this plane (Table 2). The N2 nonbonding maxima are closer (∼9%) to the N nucleus than the three bonding ones. In them, the charge simultaneously experiments the fields of both neighboring nuclei. Their final spatial position will then be determined by the competition between them. On the other hand, the nonbonded maximum does not have a second competing nucleus as a neighbor. Then, it is mainly attracted by the N nucleus and is consequently moved closer to it than the bonded maxima. These types of differences between bonding and nonbonding charge maxima in the VSCC were also found for all other amidic N atoms (Table 2).

The pyridinic nitrogen of flucytosine (N6) with its inner core and valence shell is shown in Figure 5(a). In its VSCC, one finds a nonbonding maximum corresponding to the classical "lone pair" and a bonding maximum located in the directions of each of the N6−C bonds, all placed in the molecular plane (Table 2). The nonbonding maximum in N6 VSCC has a charge concentration 16% higher than the two bonding ones and is closer (10%) to the N nucleus, as expected. The molecule also features a planar amine nitrogen (N8) with two nonbonding maxima (one above and one below the molecular plane) and three bonding ones. A bonding maximum is located in the valence shell along each of the N8−H bond directions, while the third one is along the N8−C5 direction (Table 2). All these maxima in the N8 VSCC of flucytosine are also located in the molecular plane. Charge concentrations in the valence shell of the planar amine are slightly different than those of amidic N atoms. The nonbonding maxima in the amine had smaller concentrations (11%), while the bonding ones have a slightly lower value (12%). This shows the effects on the N VSCC of bonding with atoms with slightly different electronegativities such as H and C.3,4

Charge Distribution of the F−C and C═O Bonds

The determination of the $\nabla^2\rho(\mathbf{r})$ distribution allows an analysis of bonding of the F and O to C atoms in the different molecules [Figure 5(a)−(c)]. It can be observed there that the charge distribution of F atomic basin has a peculiar shape not found in other elements. The Laplacian distribution is such that a slightly flattened spherical distribution surrounding the F nucleus coexists with a small conical one that is located in the interatomic region next to the C atom [Figure 5(a)−(c)].[3,4] This rather flat cone of charge is such that its base is near the C atom, and its axis is directed along the F−C bond direction. The valence shell of F atoms featured only two nonbonded maxima in flucytosine and 5-fluorouracil. In general, the bonding of an F with a C atom is such that it either forms a single bond with three nonbonding maxima[16,17] in its VSCC or there is conjugation that generates a finite double bond character in the F−C bond. In this latter case, only two "lone pairs" are

TABLE 2: Critical Points in the VSCC of N and O Atoms

	flucytosine							
	N2					N6		
	b	b	b	nb	nb	b	b	nb
radius	0.802	0.809	0.793	0.756	0.756	0.816	0.811	0.734
$\rho(\mathbf{r}_c)$	0.497	0.485	0.498	0.497	0.497	0.486	0.474	0.576
$\nabla^2\rho(\mathbf{r}_c)$	−2.067	−1.778	−1.955	−1.961	−1.961	−1.679	−1.695	−2.980

	O9		N8				
	nb	nb	b	b	b	nb	nb
radius	0.636	0.637	0.810	0.807	0.806	0.752	0.749
$\rho(\mathbf{r}_c)$	0.961	0.955	0.492	0.490	0.491	0.515	0.515
$\nabla^2\rho(\mathbf{r}_c)$	−6.024	−5.937	−1.799	−1.963	−1.984	−2.147	−2.147

	uracil									
	N5					N11				
	b	b	b	nb	nb	b	b	b	nb	nb
radius	0.797	0.805	0.802	0.755	0.755	0.795	0.807	0.797	0.756	0.756
$\rho(\mathbf{r}_c)$	0.500	0.488	0.491	0.503	0.503	0.502	0.486	0.493	0.500	0.500
$\nabla^2\rho(\mathbf{r}_c)$	−2.107	−1.818	−1.858	−1.996	−1.996	−2.133	−1.784	−1.885	−1.979	−1.978

	uracil								
	O9		O10		5- fluorouracil N5				
	nb	nb	nb	nb	b	b	b	nb	nb
radius	0.637	0.637	0.635	0.634	0.803	0.796	0.809	0.754	0.754
$\rho(\mathbf{r}_c)$	0.951	0.953	0.966	0.970	0.492	0.501	0.479	0.506	0.506
$\nabla^2\rho(\mathbf{r}_c)$	−5.873	−5.905	−6.159	−6.192	−1.850	−2.113	−1.752	−2.040	−2.040

	5- fluorouracil								
	N10					O8		O9	
	b	b	b	nb	nb	nb	nb	nb	nb
radius	0.794	0.806	0.800	0.756	0.756	0.637	0.637	0.634	0.635
$\rho(\mathbf{r}_c)$	0.503	0.485	0.491	0.500	0.500	0.952	0.950	0.971	0.965
$\nabla^2\rho(\mathbf{r}_c)$	−2.144	−1.787	−1.855	−1.981	−1.982	−5.886	−5.859	−6.211	−6.136

	thymine									
	N5					N10				
	b	b	b	nb	nb	b	b	b	nb	nb
radius	0.797	0.805	0.803	0.755	0.755	0.795	0.806	0.798	0.756	0.756
$\rho(\mathbf{r}_c)$	0.500	0.486	0.492	0.503	0.503	0.502	0.487	0.493	0.500	0.500
$\nabla^2\rho(\mathbf{r}_c)$	−2.099	−1.811	−1.858	−2.006	−2.003	−2.133	−1.799	−1.885	−1.973	−1.972

	O8		O9	
	nb	nb	nb	nb
radius	0.637	0.637	0.635	0.635
$\rho(\mathbf{r}_c)$	0.952	0.950	0.968	0.966
$\nabla^2\rho(\mathbf{r}_c)$	−5.887	−5.859	−6.163	−6.152

TABLE 3: Atomic Charges in Some O and C Atoms

uracil				
O9	O10	C2	C3	C4
−1.212	−1.187	1.440	−0.009	0.415
thymine				
O8	O9	C2	C3	C4
−1.214	−1.191	1.433	0.025	0.397
5-fluorouracil				
O85	O9	C2	C3	C4
−1.209	−1.165	1.476	0.566	0.438

present in the F VSCC as nonbonding maxima. They are located in the molecular plane and at ∼120 degrees from the F−C bond direction. When conjugation is present, an increase in the density and especially in the bond ellipticity is expected to occur at the BCP with respect to those of a single F−C bond. The latter seems to be the case for the F atoms in flucytosine and 5-fluorouracil (Table 1). The ϵ and $\rho(\mathbf{r}_c)$ values show a noticeable degree of double bonding in the C−F bond, a character that is 40% higher in flucytosine than in 5-fluorouracil. This shows that the resonance effect in the F−C bond in flucytosine is more important.

In the O atoms, two nonbonding charge concentrations, corresponding to the classical "lone pairs" in the carbonyl O valence shell, were found (Table 2). Such O nonbonding charge concentrations have been shown to be the sites for either protonation or H bonding.[3,4] The position of maxima in these O atoms are not all located symmetrically at 120 degrees from the C═O bond direction in the molecules studied here. If a (non)symmetrical environment were present in the immediate vicinity of the carbonyl group, then its maxima were located in

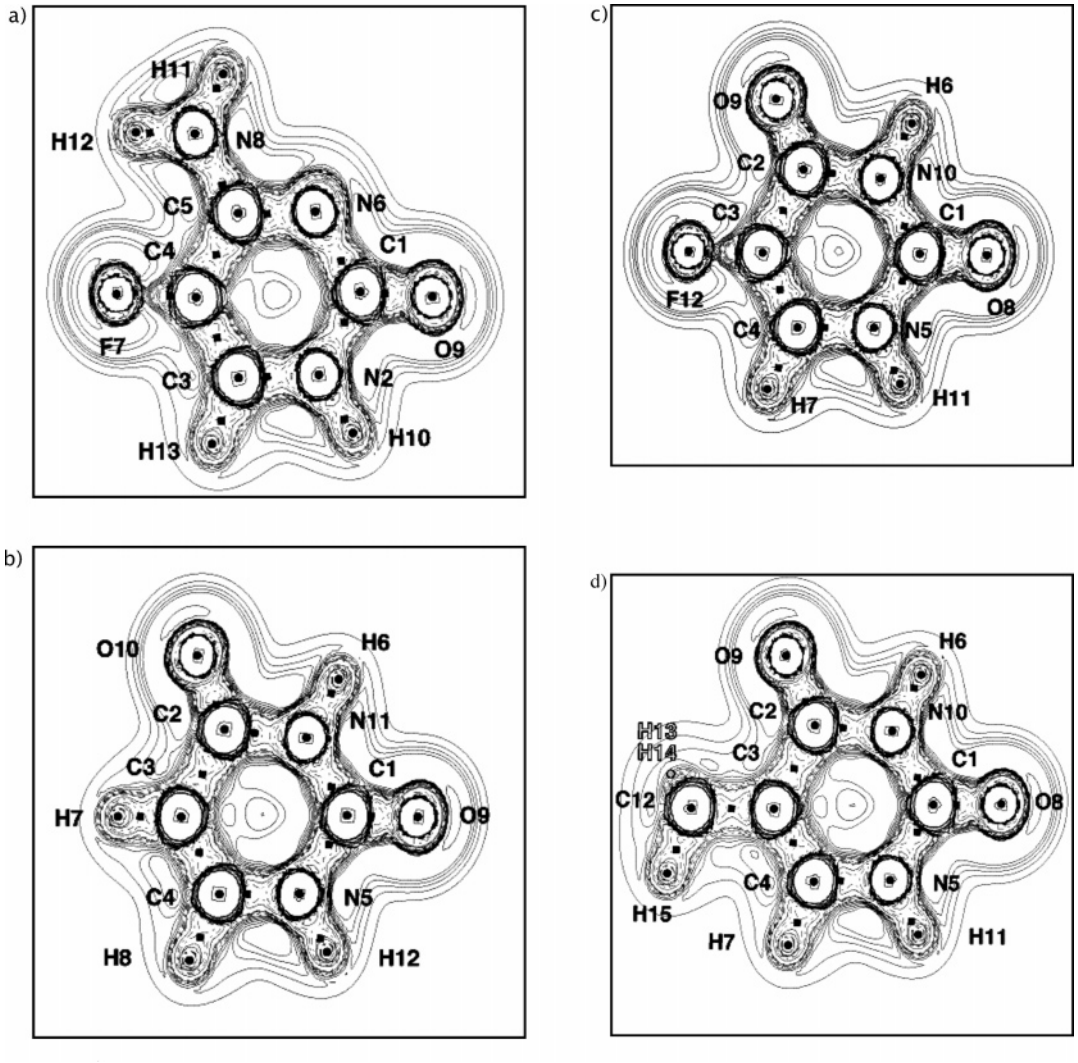

Figure 5. Laplacian of $\rho(\mathbf{r})$ in the molecular plane for (a) flucytosine (b) uracil, (c) 5-fluorouracil, and (d) thymine.

(non)symmetrical positions in the O valence shell. This shows the influence of the electric field produced by the neighboring atoms in the position of the VSCC maxima of O atoms (Table 2).

Chemical Reactivity

The surface of $\nabla^2\rho(\mathbf{r}) = 0$ has been used as an indicator of chemical reactivity of organic molecules.[3,4] Comparison of 3D contours for flucytosine and related molecules [Figure 6(a)−(d)] with others such as urea and methanal [Figure 6(e),(f)] help to understand their chemical reactivity. In these figures, the electronic core formed by closed shells is shown as a small dark spherical body centered at the nuclei for all atoms except H, which does not have such concentration. The cores may be easily seen inside the different C atoms where the valence shell shows significant regions of charge depletion. Such C atoms are engaged in bonding with O, F, or N atoms. Nevertheless, there are other C atoms in these molecules, with either a small region of charge depletion or none at all. In them, cores are inside a large and darker surface that represents the VSCC, i.e., C3 in flucytosine. Substitution of the H atoms by amine groups in methanal generates significant changes in the contour of the C atom valence shell [Figure 6(f)]. In the 3D contour plot of $\nabla^2\rho(\mathbf{r}) = 0$ one sees that the C atom in urea shows a marked increase in the area of charge depletion in its valence shell with respect to methanal. In the latter, there is a residual volume of charge in the shell that connects both H atoms,[4] while in urea these regions disappear altogether and a noticeable gap is now present in the C atom VSCC [Figure 6(e)]. Similar changes were found for part of the valence shell of the C atom in the carbonyl group of flucytosine (C1) and related molecules. All amide-forming Cs had VSCCs similar to that of such an atom in urea [Figure 6(e)]. Nevertheless, some of these C atoms had valence shells with bridging connections left between charge concentrations of neighboring bonds, i.e., C2 from uracil and C2 from 5-fluorouracil.

The regions of charge depletion in the VSCC of the C atom have been identified with sites of nucleophilic attack in methanal and similar compounds.[4,18] Therefore, it seems that the carbonyl groups in our set of molecules are candidates for such a type of attack. C atoms with the largest depression in their VSCC will be the most prone to this type of nucleophilic attack.[18,19] The other C atoms of the carbonyl groups showed a diminished capability for such an attack because they have a smaller region of charge depression in their VSCC to be filled.

C4 atoms presented holes in their valence shell (uracil> thymine) [Figure 6(b)−(d)]. This was not a general trend as such holes were absent in flucytosine or present only in a small fashion in 5-fluorouracil [Figure 6(a),(c)]. It seems plausible that in the latter molecules, the charge in C4 may not be shifted toward the neighboring N because of the attraction generated by the neighboring F atom. When an electron-donating atom

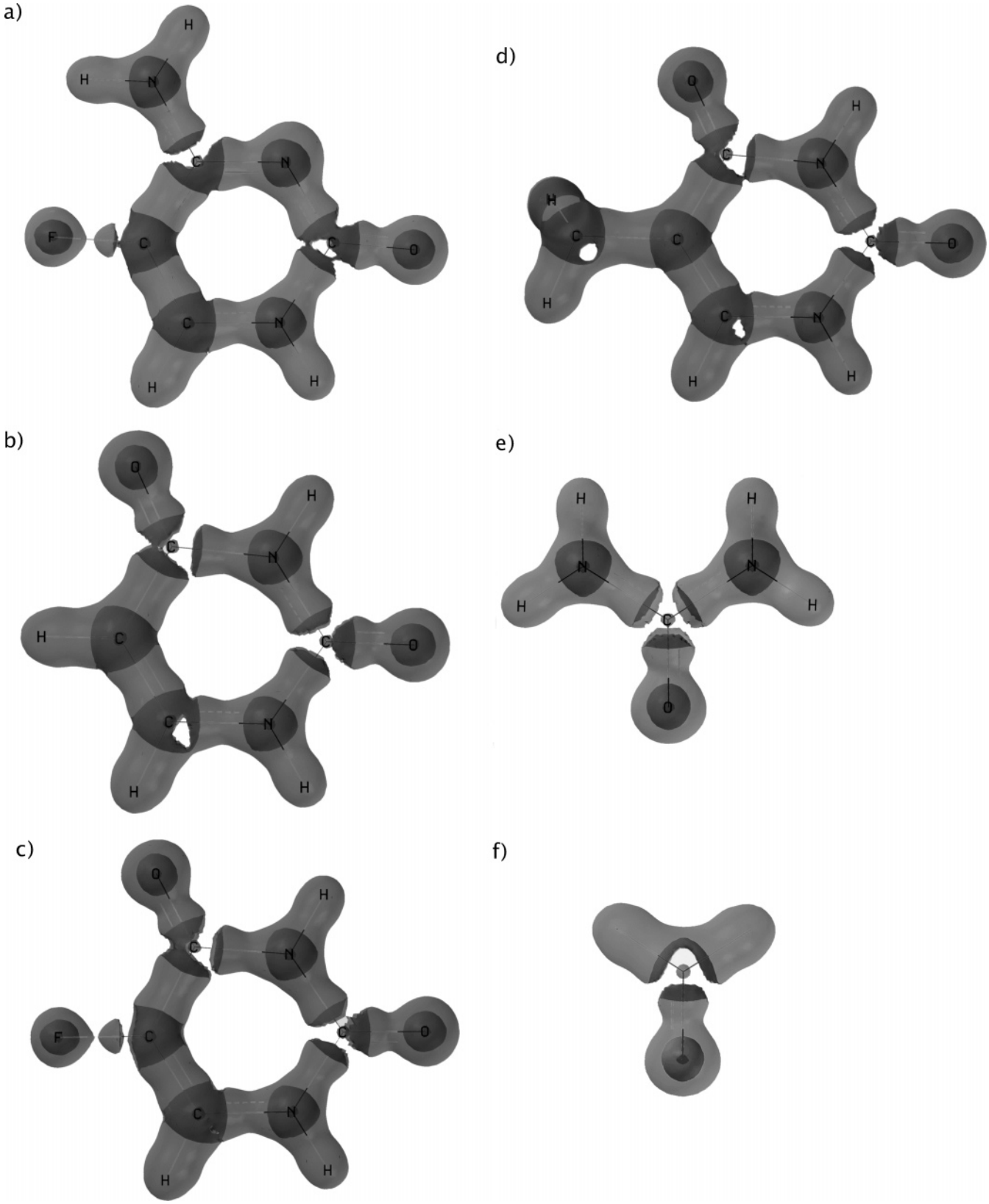

Figure 6. Surfaces of $\nabla^2\rho(\mathbf{r}) = 0$ for (a) flucytosine, (b) uracil, (c) 5-fluorouracil, (d) thymine, (e) urea, and (f) methanal.

(H) or group ($-CH_3$) replaces F, the N atom is now capable of attracting more charge from the neighboring C, leading to the production of holes in the valence shell of C4.

Conclusions

The use of the $\rho(\mathbf{r})$ topology allows a characterization of electronic distribution and chemical reactivity of flucytosine and related molecules employing only BCP vectors, net atomic charges $q(\Omega)$, and the distribution of $\nabla^2\rho(\mathbf{r}_c)$. Chemical bonds were characterized through vectors formed with $\rho(\mathbf{r})$ and $\nabla^2\rho(\mathbf{r})$ and bond ellipticity ϵ calculated at the BCPs. It was found that these vectors were all quite similar within each set of C═O, C−H, and N−H bonds. The C−C bonds formed three different sets: one with a significant degree of double bonding,

a second one corresponding to single C−C bonds with a finite ellipticity produced by conjugation/hyperconjugation, and a third one representing a pure single bond ($C-CH_3$) present in thymine. In N−C bonds, an increase in $\rho(\mathbf{r}_c)$ at the BCP produced by a decrease in bond length (an increase in the double bond character) was not reflected in an increased ellipticity, as found in all the C−C bonds of the molecules studied in this work and in some F derivatives of AZT. This shows, again, that the bond ellipticity is not a reliable measure of bond order. Even if the $\rho(\mathbf{r}_c)$ and $\nabla^2\rho(\mathbf{r}_c)$ values were fairly constant within atomic groups such as the carbonyls, the neighboring atoms influenced the ellipticity at the BCPs. The $\nabla^2\rho(\mathbf{r})$ distribution suggested several bonding and nonbonding maxima in the valence shell of N, O, and F, while only bonding ones were detected in all the C atom shells. The VSCC of F showed a slightly flattened spherical distribution with a conical one located in the interatomic region. Only two nonbonding maxima ("lone pairs") were found in the VSCC of the F atoms. This was a result of the noticeable degree of double bonding found for the F−C bonds. The existence of nonbonding maxima in the VSCC of the different atoms except H indicated the sites for electrophilic attack and H bonding, present in these molecules. The determination of the $\nabla^2\rho(\mathbf{r}_c)$ distribution also allowed the identification of regions in the valence shell of the C atoms, prone to nucleophilic attack. C atoms of the different molecules showed different degrees of charge depletion in the VSCC that leads to this attack. Such differences seemed related to the presence of electron accepting atoms such as N or O next to the C atom.

Acknowledgment. Thanks to Fondo Nacional de Ciencia y Tecnología (FONACIT), Venezuela, for Grant G97-000615 and to P.L.A. Popelier from University of Manchester, U.K., for kindly providing the Morphy 95 and 98 programs.

References and Notes

(1) Vermes, A.; Guchelaar, H. J.; Dankert, J. *J. Antimicrob. Chemother.* **2000**, *46*, 171−179.

(2) Hope, W. W.; Tabernero, L.; Denning, D. W.; Anderson, M. J. *Antimicrob. Agents Chemother.* **2004**, *48*, 4377−4386.

(3) Bader, R. F. W. *Atoms in Molecules: A Quantum Theory*; Clarendon: Oxford, U.K., 1990.

(4) Popelier, P. L. A. *Atoms in Molecules: An Introduction*; Prentice Hall: Edinburgh, 2000.

(5) Leach, A. R. *Molecular Modelling*, 2nd ed.; Prentice Hall: London, 2001.

(6) *GaussView03M*; Gaussian Inc.: Pittsburgh, PA. Frisch, M. J.; Trucks, G. W.; Schlegel, H. B.; Scuseria, G. E.; Robb, M. A.; Cheeseman, J. R.; Montgomery, J. A., Jr.; Vreven, T.; Kudin, K. N.; Burant, J. C.; Millam, J. M.; Iyengar, S. S.; Tomasi, J.; Barone, V.; Mennucci, B.; Cossi, M.; Scalmani, G.; Rega, N.; Petersson, G. A.; Nakatsuji, H.; Hada, M.; Ehara, M.; Toyota, K.; Fukuda, R.; Hasegawa, J.; Ishida, M.; Nakajima, T.; Honda, Y.; Kitao, O.; Nakai, H.; Klene, M.; Li, X.; Knox, J.; Hratchian, H. P.; Cross, J. B.; Adamo, C.; Jaramillo, J.; Gomperts, R.; Stratmann, R. E.; Yazyev, O.; Austin, A. J.; Cammi, R.; Pomelli, C.; Ochterski, J. W.; Ayala, P. Y.; Morokuma, K.; Voth, G. A.; Salvador, P.; Dannenberg, J. J.; Zakrzewski, V. G.; Dapprich, S.; Daniels, A. D.; Strain, M. C.; Farkas, O.; Malick, D. K.; Rabuck, A. D.; Raghavachari, K.; Foresman, J. B.; Ortiz, J. V.; Cui, Q.; Baboul, A. G.; Clifford, S.; Cioslowski, J.; Stefanov, B. B.; Liu, G.; Liashenko, A.; Piskorz, P.; Komaromi, I.; Martin, R. L.; Fox, D. J.; Keith, T.; Al-Laham, M. A.; Peng, C. Y.; Nanayakkara, A.; Challacombe, M.; Gill, P. M. W.; Johnson, B.; Chen, W.; Wong, M. W.; Gonzalez, C.; Pople, J. A. *Gaussian O3M, Revision B.04*; Gaussian, Inc.: Pittsburgh, PA, 2003.

(7) *Morphy 95*: Popelier, P. L. A. *Comput. Phys. Commun.* **1996**, *93*, 212−218.

(8) *Morphy 98*, a topological analysis program written by P. L. A. Popelier with a contribution from R. G. A. Bone (UMIST, England, EU).

(9) *PROAIM*: Biegler-König, F. W.; Bader, R. F. W.; Tang, T. *J. Comput. Chem.* **1982**, *13*, 317−328.

(10) Gillespie, R. J.; Popelier, P. L. A. *Chemical Bonding and Molecular Geometry*; Oxford University Press: Oxford, 2001.

(11) Popelier, P. L. A. *J. Phys. Chem. A* **1999**, *103*, 2883−2890.

(12) Topsom, R. D. *Acc. Chem. Res.* **1983**, *16*, 292−298.

(13) Bader, R. F. W.; See, T. S.; Cremer D.; Kraka, E. *J. Am. Chem. Soc.* **1983**, *105*, 5061−5068.

(14) Fidanza, N. G.; Sosa, G. L.; Lobayan, R. M.; Peruchena, N. M. *J. Mol. Struct: THEOCHEM* **2005**, *722*, 65−78.

(15) Fradera, X.; Austen, M. A.; Bader, R. F. W. *J. Phys. Chem. A* **1999**, *103*, 304−314.

(16) Castillo, N.; Boyd, R. J. *Chem. Phys. Lett.* **2005**, *403*, 47−54.

(17) Bach, A.; Lentz, D.; Luger, P. *J. Phys. Chem. A* **2001**, *105*, 7405−7412.

(18) Carroll, M. T.; Cheeseman, J. R.; Osman, R.; Weinstein, H. *J. Phys. Chem.* **1989**, *93*, 5120−5123.

(19) Mosquera, R. A.; Graña, A. M. *Rec. Res. Dev. Chem. Phys.* **2001**, *2*, 23−36.